Efficient bilayer polymer solar cells possessing planar mixed-heterojunction structures†

Jen-Hsien Huang,[a] Kuang-Chieh Li,[b] Dhananjay Kekuda,[a] Hari Hara Padhy,[b] Hong-Cheu Lin,[b] Kuo-Chuan Ho[c] and Chih-Wei Chu*[ad]

We have investigated the influence of thermal annealing on the performance of polymer bilayer solar cell devices incorporating poly{2,6-(4,4-bis[2-ethylhexyl]-4H-cyclopenta[2,1-b;3,4-b′]dithiophene)-alt-4,7-(2,1,3-benzothiadiazole)} (PCPDTTBT) as the donor and two kinds of fullerenes (C_{60}, C_{70}) as acceptors. The higher absorption of C_{70} increased the external quantum efficiency in the spectral range 400–600 nm. We observed morphological changes of the polymer films when the pre-annealing temperature was near the crystalline temperature (T_c, 207 °C). These nanostructural transformations resulted in a modified interfacial morphology of the donor phases and, therefore, greatly influenced the device performance. Post-annealing treatment reorganized the interface between the donor and acceptor phases, leading to better contact. The highest power conversion efficiency (2.85%) was obtained when we performed device pre- and post-annealing both at 200 °C for 30 min; the open-circuit voltage was 0.69 V and the short-circuit current was 8.42 mA cm^{-2}.

1. Introduction

In recent years, polymer-based solar cells have become increasingly attractive as a means of harnessing clean energy because of their low cost,[1–4] ease of processing,[5–8] and the feasibility of fabricating them on various substrates. Since the bilayer heterojunction concept was proposed in 1986 by Tang et al.,[9] many advances in bilayer solar cells has been achieved through the use of various material combinations.[10–15] Although bilayer devices can exhibit good charge transport,[16] their power conversion efficiencies (PCEs) are limited by the small interface between the electron donor and acceptor.[17] Moreover, the short exciton diffusion lengths of the organic materials [ca. 6.8–8.5 nm for poly(3-hexylthiophene) (P3HT)[18] and ca. 40 nm for fullerene (C_{60})[19]] restrict the thickness of the active layer, leading to inefficient absorbance. To overcome these problems, Heeger et al. proposed the use of bulk heterojunction (BHJ) solar cells, which mix the donor and acceptor components in a bulk volume so that a donor–acceptor interface is located within a distance less than the exciton diffusion length of each absorbing site.[20] Although the exciton dissociation efficiencies for these blend structures are high relative to those of bilayer structures, several problems are typically encountered within the disordered nanostructures. For example, a well-mixed blend of two semiconductors will lack the continuous channels required for charge transport, causing a significant fraction of the carriers to recombine at donor–acceptor interfaces before they have the chance to reach their respective electrodes.[21,22] In addition, phase separation between the two semiconductors can lead to the length scale for exciton dissociation becoming too great. To overcome these problems, ordered BHJs, prepared by filling an inorganic nanostructure with conjugated polymers, have been developed for the fabrication of efficient solar cells.[23] Although much research has been performed in the area of polymer/TiO₂ hybrid systems, their efficiencies are limited because of incompatibility between the nanostructure dimensions of TiO₂ and the exciton diffusion length of the polymer layers.[24–26]

Thermotropic liquid crystalline copolymers are attracting great attention in the area of organic electronics, especially for their use in thin film transistors and solar cells.[27–32] These copolymers can undergo significant morphological changes and can form periodic nanostructures if annealed at temperatures higher than their glass transition temperatures. Such transformations lead to a crystalline phase and, therefore, a dramatic increase in hole mobility. In a previous study, we developed a cyclopentadithiophene (CPDT)-based copolymer, PCPDTTBT, comprising bithiazole and thiophene units.[33] PCPDTTBT exhibited a broad absorption range and good charge-transporting properties, with a hole mobility of 5.2×10^{-4} cm² V^{-1} s^{-1}, making it a good candidate for use in high efficiency polymer solar cells. To increase the efficiency of the p–n junction interfacial area of bilayer solar cells, in this study we employed the thermotropic liquid crystalline PCPDTTBT and fullerenes to fabricate planar-mixed heterojunction solar cells. Furthermore, we also increased the absorbance of the solar cell devices by replacing C_{60}, which possesses a very low absorption coefficient in the visible spectrum, with the analogous

[a] Research Center for Applied Sciences, Academia Sinica, Taipei 11529, Taiwan. E-mail: gchu@gate.sinica.edu.tw; Fax: +886-2-2782-6680; Tel: +886-2-2789-8000 ext 70

[b] Department of Materials Science and Engineering, National Chiao Tung University, Hsinchu 300, Taiwan

[c] Department of Chemical Engineering, National Taiwan University, Taipei 10617, Taiwan

[d] Department of Photonics, National Chiao Tung University, Hsinchu 300, Taiwan

† This paper contains work presented at the 2009 International Conference on Carbon Nanostructured Materials held in Santorini, Greece.

complementary acceptor C_{70}. As a result, the planar-mixed heterojunction solar cells satisfied several requirements simultaneously: a high-area heterojunction interface, a large absorbance, and good charge transfer. We suspect that devices based on this type of structure might one day rival the performance of BHJ solar cells.

2.   Experimental

PCPDTTBT was synthesized according to a previously published procedure.[33] The fabrication process of the devices was initiated by cleaning the indium tin oxide (ITO)-coated glass. The cleaned substrates were exposed to UV ozone for 15 min. Poly(3,4-ethylenedioxythiophene):poly(styrene sulfonate) (PEDOT:PSS) was then spun onto the ITO substrates, which were subsequently dried at 120 °C for 1 h. The active layer consisted of two layers. First, a copolymer layer was deposited through spin coating. A solution of PCPDTTBT polymer (10 mg mL^{-1}, 1 wt%) in 1,2,4-trichlorobenzene was spun on the substrates at 2500 rpm for 60 s. The films were then annealed at various temperatures (100 to 250 °C) for 1 h to modify their morphologies. The samples were then patterned through a suitable mask and transferred to a vacuum chamber, where n-type fullerene C_{70} was deposited. The deposition rate and thickness of the fullerene (C_{60} or C_{70}) thin films were 0.5 Å s^{-1} and 40 nm, respectively, in each case. After deposition of the active layer, Al cathodes were deposited. The surface morphologies were visualized using atomic force microscopy (AFM). X-Ray diffraction was used to measure the crystallinity of the films. The optical absorption spectra of the PCPDTTBT films were recorded at room temperature using a UV–Vis spectrophotometer (V-650, Jasco). The external quantum efficiency (EQE) was measured using a lock-in detector and monochromatic light from a Xe lamp. The

photoluminescence (PL) spectra were obtained using a Hitachi F-4500 instrument. The illuminated current–voltage (J–V) characteristics were studied using an Agilent 4056 semiconductor parameter analyzer.

3.   Results and discussion

Fig. 1 presents the molecular structure of the low-bandgap polymer and a schematic energy level diagram of the highest occupied molecular orbital (HOMO) and lowest unoccupied molecular orbital (LUMO) of PCPDTTBT relative to those of the fullerenes. All photovoltaic devices were fabricated with a bilayer structure (Fig. 1c); the thicknesses of the polymer and fullerene layers were held constant at 100 and 40 nm, respectively.

Fig. 2 displays the absorption spectra of the pure PCPDTTBT, PCPDTTBT/C_{60}, and PCPDTTBT/C_{70} films. These films were all obtained by spin-coating PCPDTTBT onto ITO glass and then thermally depositing the fullerenes. The spectrum of the PCPDTTBT film reveals an absorption maximum at 560 nm, with its absorption onset at 660 nm. The absorption of PCPDTTBT between 350 and 550 nm was complemented by combining PCPDTTBT with C_{60}. The absorbance of C_{70} is much greater than that of C_{60} (inset to Fig. 2) because of its much higher absorption coefficient. The low absorption coefficient of C_{60} arises from its high degree of symmetry, which forbids lowest-energy transitions. Therefore, the absorbance of PCPDTTBT/C_{70} was much higher than that of PCPDTTBT/C_{60}. This phenomenon is also clearly evident in the photographs presented in Fig. 2.

Fig. 3 reveals the performances of the bilayer solar cells fabricated from PCPDTTBT/C_{60} and PCPDTTBT/C_{70}. These devices were both pre- and post-annealed at 150 °C. The short
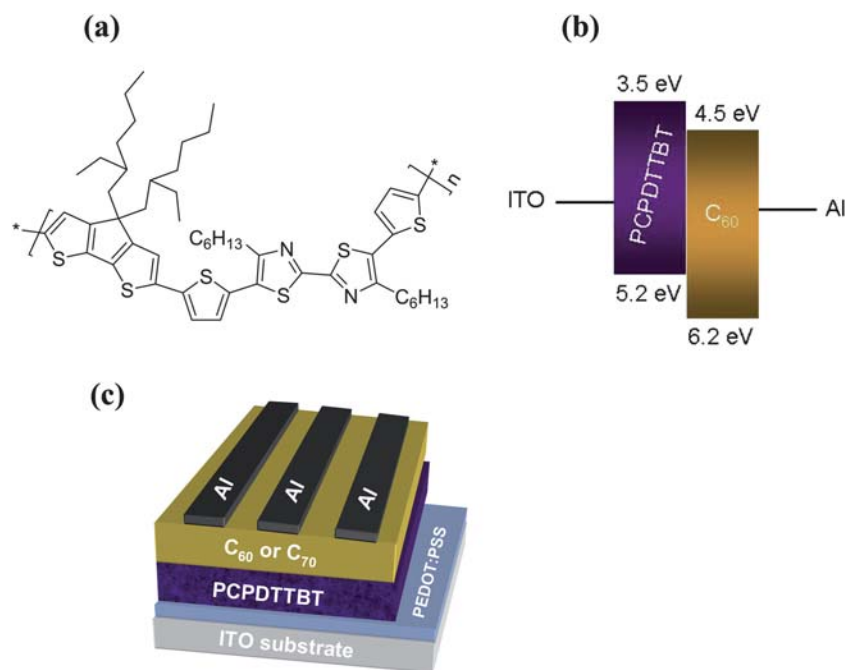

Fig. 1 (a) Molecular structure of PCPDTTBT. (b) HOMO and LUMO energy levels of PCPDTTBT and the fullerenes. (c) Schematic representation of the structure of the bilayer solar cells.
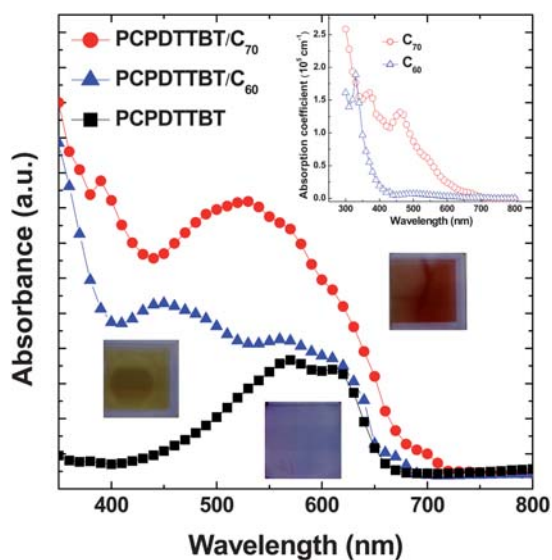
Fig. 2 Optical absorption spectra of the pure PCPDTTBT, PCPDTTBT/C_{60}, and PCPDTTBT/C_{70} films. Inset: Absorption coefficients of C_{60} and C_{70}.
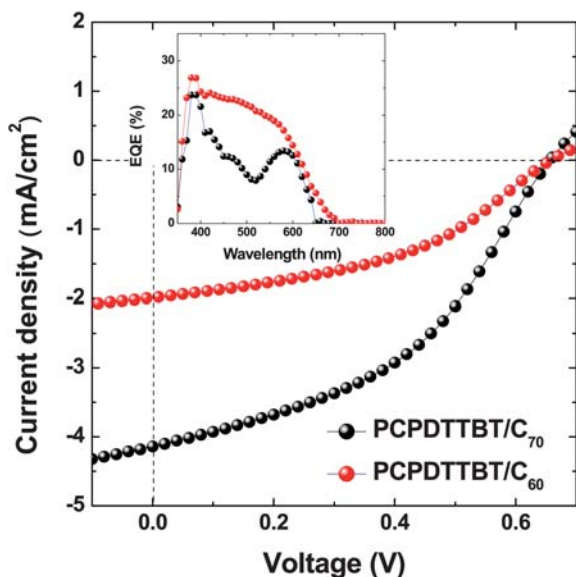

Fig. 3 Performance of solar cells incorporating PCPDTTBT/C_{60} and PCPDTTBT/C_{70}. The pre- and post-annealing temperatures were both 150 °C.

circuit current (J_{SC}) and fill factor (FF) of the PCPDTTBT/C_{60}-based device were 1.99 mA cm^{-2} and 42.8%, respectively; combined with an open circuit voltage (V_{OC}) of 0.66 V, it delivered a PCE of 0.56%. The photocurrent underwent a significant increase after replacing C_{60} with C_{70}. Under a light intensity of 100 mW cm^{-2}, the value of J_{SC} increased up to 4.13 mA cm^{-2}—an enhancement of greater than a 107% over that obtained for the PCPDTTBT/C_{60}-based device. This behavior can be explained by considering the much larger absorbance of C_{70} relative to that of C_{60}. As a result, the PCPDTTBT/C_{70}-based device exhibited a PCE of 1.17%. The EQE (inset to Fig. 3) also exhibited a higher photoresponse between 400 and 600 nm

for the PCPDTTBT/C_{70}-based device. These results are in good agreement with the UV–Vis spectra.

Fig. 4 displays the J–V characteristics of the photovoltaic devices that had undergone pre-annealing at various temperatures and subsequent post-annealing at 150 °C after cathode deposition. The pre-annealing temperature mainly affected the value of J_{SC}, with the value of V_{OC} remaining largely unchanged, except for the device annealed at 250 °C. As a consequence, the photocurrent increased continuously from 3.51 to 6.46 mA cm^{-2} upon increasing the pre-annealing temperature from 100 to 200 °C. Because PCPDTTBT possessed a value of T_c of 207 °C,[33] its polymer chains underwent higher ordering at higher temperatures. This behavior can result in enhanced polymer chain stacking and a rougher morphology. Therefore, the devices
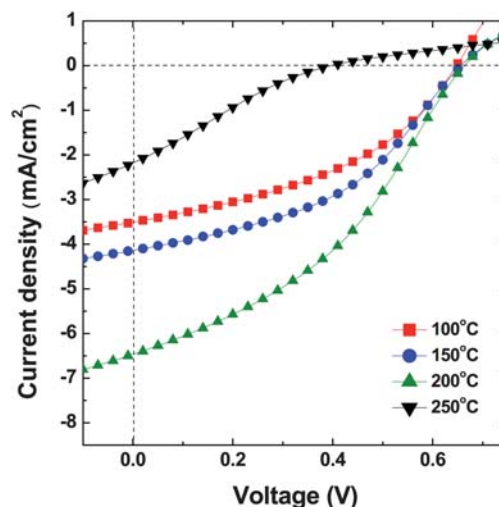

Fig. 4 J–V curves of PCPDTTBT/C_{70}-based bilayer solar cells fabricated at various pre-annealing temperatures.
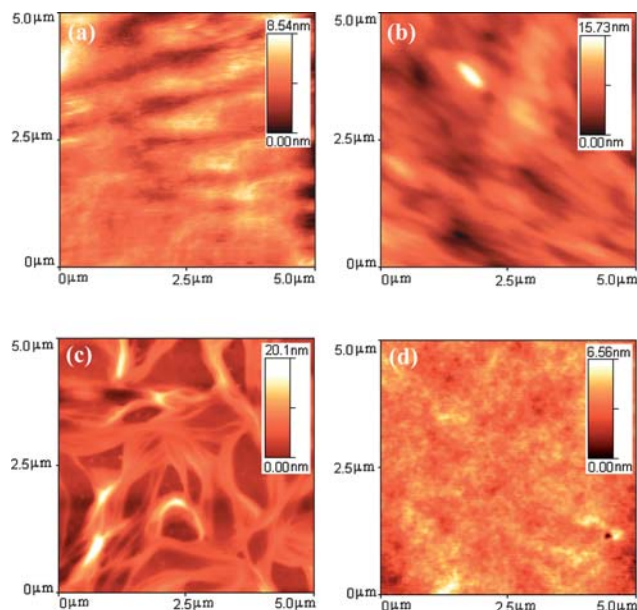

Fig. 5 Tapping mode AFM images of PCPDTTBT films that had been subjected to pre-annealing at (a) 100, (b) 150, (C) 200, and (d) 250 °C.

displayed superior performance after pre-annealing. The optimized photovoltaic device, which had been pre-annealed at 200 °C (Fig. 4), exhibited a value of J_{SC} of 6.46 mA cm^{-2}, a value of V_{OC} of 0.67 V, and a FF of 38.2%.

In view of the importance of the interfacial morphology of solar cell devices, we used AFM to investigate the surface morphology of the annealed PCPDTTBT surfaces (Fig. 5). After annealing at 100 °C, the polymer film was smooth and featureless. As the annealing temperature increased, the surface roughness increased accordingly (Fig. 5b and c). After annealing at 200 °C, distorted fibrils having a characteristic width scale of *ca.* 100 nm were evident in the polymer film. This temperature is quite close to the value of T_c (207 °C) of PCPDTTBT. Therefore, we consider the distortion arose in part from the thermally induced crystallinity of PCPDTTBT. The morphology returned to a featureless smooth surface, however, after increasing the annealing temperature to 250 °C—that is, when the annealing temperature was higher than the melting temperature (T_m, 237 °C)[33] of PCPDTTBT, causing it to melt. These images reveal that an annealing temperature between 150 and 200 °C resulted in a rougher morphology. Subsequent deposition of C$_{70}$ onto the fibrillar structure led, therefore, to a well-mixed interface between PCPDTTBT and C$_{70}$. Such planar-mixed heterojunction devices feature a larger interfacial area for exciton dissociation, relative to that of a conventional bilayer structure; as a result, a greater photocurrent can be generated.

We also monitored the polymer structures using XRD. Fig. 6 presents XRD spectra of the PCPDTTBT films annealed at various temperatures. Again, the XRD spectrum of the PCPDTTBT film annealed at 200 °C exhibited a dramatic increase in intensity of the peak at a value of 2θ of 6.2° (corresponding to the interchain spacing in PCPDTTBT associated with interdigitated alkyl chains). This finding suggests that the polymer underwent chain-reorganization and self-assembly during the annealing process. Because greater stacking of polymer chains can improve charge mobility, the polymer film annealed at 200 °C not only possessed a favorable morphology but also enhanced charge mobility—two positive effects for improving solar cell efficiency.
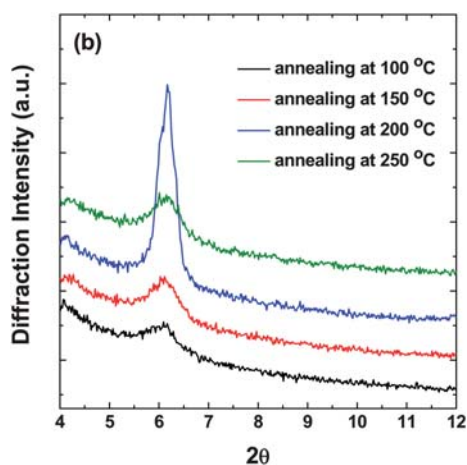
Fig. 7 displays the *J–V* and EQE characteristics under illumination for photovoltaic devices that had undergone pre-annealing at 200 °C and subsequent post-annealing at various temperatures after cathode deposition. All the performance parameters for the planar-mixed heterojunction device as a function of pre- and post- annealing temperatures are summarized in Table 1. We observe that the cell performance was improved further after post-treatment. The value of J_{SC} and the FF were both enhanced upon increasing the post-annealing temperature, with a temperature of 200 °C providing the best efficiency (up to 2.85%). We find the performance of the planar-mixed heterojunction device can rival those of the soluble-processed BHJ cell.[33] Ayzner *et al.* also reported that BHJ geometry is not necessary for high efficiency, and bilayer solar cells can be nearly as efficient as BHJ solar cells.[34] Consistent with the trend in the value of J_{SC}, the EQE magnitude initially decreased slightly from 60.0% (post-annealed at 200 °C) to 54.6% (post-annealed at 150 °C), followed by a rapid decrease to 26.7% for the device subjected to a post-annealing temperature of 250 °C. The reason for the superior performance of the devices after
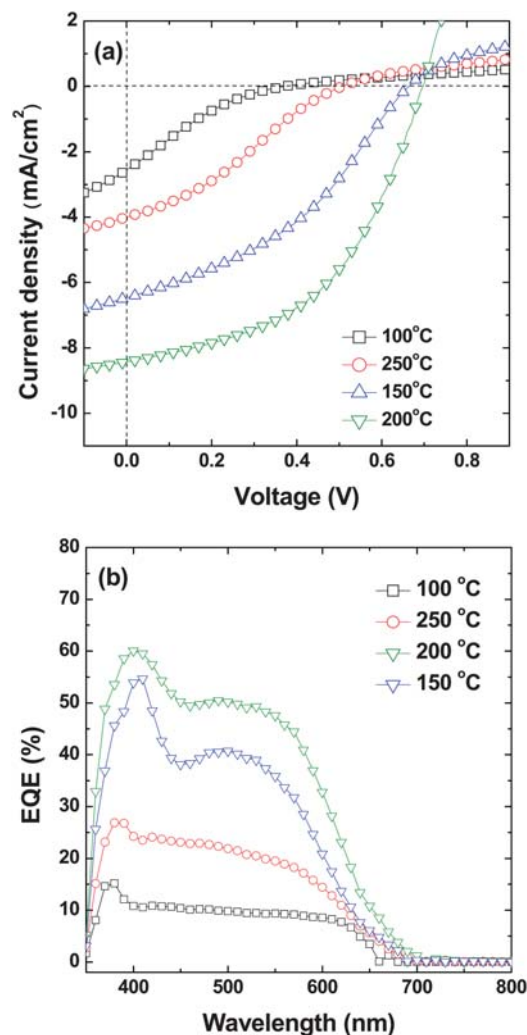

Fig. 6 XRD spectra of PCPDTTBT films that had been annealed at various temperatures.

Fig. 7 (a) *J–V* curves and (b) EQE spectra of PCPDTTBT/C$_{70}$-based bilayer solar cells that had been subjected to various post-annealing temperatures. The pre-annealing temperature was held constant at 200 °C.

Table 1 A summary of the cell performance as a function of pre- and post-annealing temperatures

Condition	J_{SC}/mA cm^{-2}	V_{OC}/V	FF (%)	PCE (%)
Pre-annealing[a]				
100 °C	3.51	0.65	41.2	0.94
150 °C	4.14	0.65	43.4	1.17
200 °C	6.46	0.66	38.7	1.65
250 °C	2.18	0.39	22.3	0.19
Post-annealing[b]				
100 °C	2.55	0.38	17.5	0.17
150 °C	6.46	0.66	38.7	1.65
200 °C	8.42	0.70	48.4	2.85
250 °C	4.01	0.51	29.8	0.61

[a] The post-annealing temperature was controlled at 150 °C for 1 h. [b] The pre-annealing temperature was controlled at 200 °C for 1h.

post-annealing can be explained by considering the elimination of voids between the PCPDTTBT and C_{70} phases and the creation of a larger interface for exciton dissociation.[35] This also can be explained by the shape of J–V curves. For the devices annealed at a temperature lower than 200 °C, an inflection point (S-shape) can be seen. The S-shape is often observed when solar cell devices have a barrier to carrier transport.[36–39] These phenomena are further supported by the PL emission spectra. Fig. 8 reveals that excitons were not fully quenched in the bilayer structure, indicating a poor interface between the PCPDTTBT and C_{70} phases. Although the pre-annealing process did roughen the morphology of PCPDTTBT, leading to a planar-mixed heterojunction interface, the fibrillar surface also resulted in some of the deposited C_{70} molecules not touching the underlying PCPDTTBT; such defects at the interface reduced the exciton dissociation efficiency. This problem was overcome after post-annealing to reorder the polymer and C_{70} phases. Therefore, the PL emission decreased upon increasing the post-annealing temperature. The thermal annealing process enabled spatial

rearrangement of the polymer chains and C_{70}, thereby improving contact between the donor and acceptor layers.

4. Conclusion

We have fabricated thermally induced, planar mixed-heterojunction solar cells based on PCPDTTBT and fullerenes. Pre-annealing led to a thermally induced fibrillar morphology that increased the interfacial area between the donor and acceptor phases. Post-annealing reorganized the interface between the donor and acceptor phases to enhance their contact area. The optimal annealing temperature was 200 °C for both pre- and post-annealing, yielding a PCE of 2.85%. Such processing treatment might be attractive for other light harvesting materials, such as thermotropic liquid crystal polymers, whose morphologies are significantly modulated through thermal treatment.

References

1 F. C. Krebs, M. Jørgensen, K. Norrman, O. Hagemann, J. Alstrup, T. D. Nielsen, J. Fyenbo, K. Larsen and J. Kristensen, *Sol. Energy Mater. Sol. Cells*, 2009, **93**, 422.
2 F. C. Krebs, S. A. Gevorgyan and J. Alstrup, *J. Mater. Chem.*, 2009, **19**, 5442.
3 F. C. Krebs, *Org. Electron.*, 2009, **10**, 761.
4 F. C. Krebs, S. A. Gevorgyan, B. Gholamkhass, S. Holdcroft, C. Schlenker, M. E. Thompson, B. C. Thompson, D. Olson, D. S. Ginley, S. E. Shaheen, H. N. Alshareef, J. W. Murphy, W. J. Youngblood, N. C. Heston, J. R. Reynolds, S. Jia, D. Laird, S. M. Tuladhar, J. G. A. Dane, P. Atienzar, J. Nelson, J. M. Kroon, M. M. Wienkm, R. A. J. Janssenm, K. Tvingstedt, F. Zhang, M. Andersson, O. Inganäs, M. Lira-Cantu, R. deBettignies, S. Guillerez, T. Aernouts, D. Cheyns, L. Lutsen, B. Zimmermann, U. Würfel, M. Niggemann, H. F. Schleiermacher, P. Liska, M. Grätzel, P. Lianos, E. A. Katz, W. Lohwasser and B. Jannonw, *Sol. Energy Mater. Sol. Cells*, 2009, **93**, 1968.
5 M. Jørgensen, K. Norrman and F. C. Krebs, *Sol. Energy Mater. Sol. Cells*, 2008, **92**, 686.
6 F. C. Krebs, *Sol. Energy Mater. Sol. Cells*, 2009, **93**, 394.
7 T. Ameri, G. Dennler, C. Lungenschmied and C. J. Brabec, *Energy Environ. Sci.*, 2009, **2**, 347.
8 M. Helgesen, R. Søndergaard and F. C. Krebs, *J. Mater. Chem.*, 2010, **20**, 36.
9 A. J. Tang, *Appl. Phys. Lett.*, 1986, **48**, 183.
10 B. Verret, S. Schols, D. Cheyns, B. P. Rand, H. Gommans, T. Aernouts, P. Heremans and J. Genoe, *J. Mater. Chem.*, 2009, **19**, 5295.
11 L. Chen, Y. Tang, X. Fan, C. Zhang, Z. Chu, D. Wang and D. Zou, *Org. Electron.*, 2009, **10**, 724.
12 B. Homa, M. Andersson and O. Inganäs, *Org. Electron.*, 2009, **10**, 501.
13 P. Sullivan and T. S. Jones, *Org. Electron.*, 2008, **9**, 656.
14 S. A. McClure, B. J. Worfolk, D. A. Rider, R. T. Tucker, J. A. M. Fordyce, M. D. Fleischauer, K. D. Harris and M. J. Brett, *ACS Appl. Mater. Interfaces*, DOI: 10.1021/am900659v.
15 M. Nakamura, C. Yang, E. Zhou, K. Tajima and K. Hashimoto, *ACS Appl. Mater. Interfaces*, 2009, **1**, 2703.
16 D. M. Stevens, Y. Qin, M. A. Hillmyer and C. D. Frisbie, *J. Phys. Chem. C*, 2009, **113**, 11408.
17 H. Xi, Z. Wei, Z. Duan, W. Xu and D. Zhu, *J. Phys. Chem. C*, 2008, **112**, 19934.
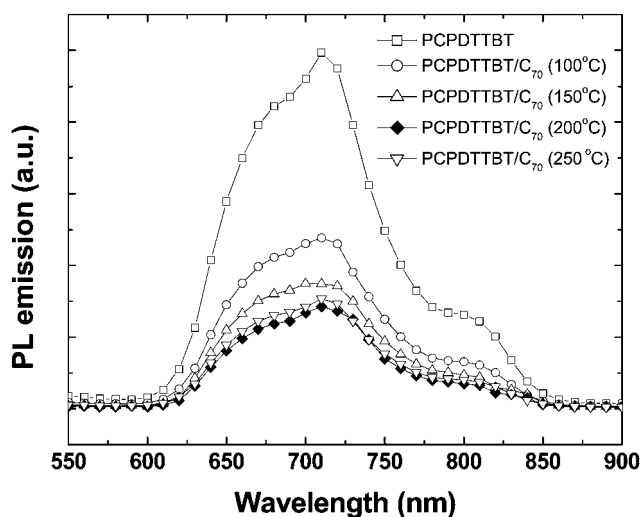18 J. E. Kroeze, T. J. Savenije, M. J. W. Vermeulen and J. M. Warman, *J. Phys. Chem. B*, 2003, **107**, 7696.

Fig. 8 PL spectra of PCPDTTBT/C_{70} bilayer films that had been subjected to various post-annealing temperatures. The pre-annealing temperature was held constant at 200 °C.

19 P. Peumans, A. Yakimov and S. R. Forrest, *J. Appl. Phys.*, 2003, **93**, 3693.
20 G. Yu, J. Gao, J. C. Hummelen, F. Wudl and A. J. Heeger, *Science*, 1995, **270**, 1789.
21 S. van Bavel, E. Sourty, G. de With, S. Veenstra and J. Loos, *J. Mater. Chem.*, 2009, **19**, 5388.
22 B. Y. Yu, W. C. Lin, J. H. Huang, C. W. Chu, Y. C. Lin, C. H. Kuo, S. H. Lee, K. T. Wong, K. C. Ho and J. J. Shyue, *Anal. Chem.*, 2009, **81**, 8936.
23 M. D. McGehee, *MRS Bull.*, 2009, **34**, 95.
24 K. M. Coakley and M. D. McGehee, *Appl. Phys. Lett.*, 2003, **83**, 3380.
25 S. S. Williams, M. J. Hampton, V. Gowrishankar, I. K. Ding, J. L. Templeton, E. T. Samulski, J. M. DeSimone and M. D. McGehee, *Chem. Mater.*, 2008, **20**, 5229.
26 Y. J. Lee, M. T. Lloyd, D. C. Olson, R. K. Grubbs, P. Lu, R. J. Davis, J. A. Voigt and J. W. P. Hsu, *J. Phys. Chem. C*, 2009, **113**, 15778.
27 J. Bouclé, P. Ravirajan and J. Nelson, *J. Mater. Chem.*, 2007, **17**, 3141.
28 M. C. Gather and D. D. C. Bradley, *Adv. Funct. Mater.*, 2007, **17**, 479.
29 J. H. Huang, C. Y. Yang, Z. Y. Ho, D. Kekuda, M. C. Wu, F. C. Chien, P. Chen, C. W. Chu and K. C. Ho, *Org. Electron.*, 2009, **10**, 27.
30 J. H. Huang, Z. Y. Ho, D. Kekuda, Y. Chang, C. W. Chu and K. C. Ho, *Nanotechnology*, 2009, **20**, 025202.
31 Q. Sun, K. Park and L. Dai, *J. Phys. Chem. C*, 2009, **113**, 7892.
32 W. Tang, V. Chellappan, M. Liu, Z. K. Chen and L. Ke, *ACS Appl. Mater. Interfaces*, 2009, **1**, 1467.
33 K. C. Li, J. H. Huang, Y. C. Hsu, P. J. Huang, C. W. Chu, J. T. Lin, K. C. Ho and K. C. Lin, *Macromolecules*, 2009, **42**, 3681.
34 A. L. Ayzner, C. J. Tassone, S. H. Tolbert and B. J. Schwartz, *J. Phys. Chem. C*, 2009, **113**, 20050.
35 J. H. Huang, Z. Y. Ho, T. H. Kuo, D. Kekuda, C. W. Chu and K. C. Ho, *J. Mater. Chem.*, 2009, **19**, 4077.
36 M. Glatthaar, M. Riede, N. Keegan, K. Sylvester-Hvid, B. Zimmermann, M. Niggemann, A. Hinsch and A. Gombert, *Sol. Energy Mater. Sol. Cells*, 2007, **91**, 390.
37 F. C. Krebs and K. Norrman, *Progr. Photovolt.: Res. Appl.*, 2007, **15**, 697.
38 M. Vogel, S. Doka, C. Breyer, M. C. L. Steiner and K. Fostiropoulos, *Appl. Phys. Lett.*, 2006, **89**, 163501.
39 S. T. Zhang, Y. C. Zhou, J. M. Zhao, Z. J. Wang, Y. Wu, X. M. Ding and X. Y. Hou, *Appl. Phys. Lett.*, 2006, **89**, 043502.